

## Fabrication of high-aspect-ratio polymer-based electrostatic comb drives using the hot embossing technique

To cite this article: Yongjun Zhao and Tianhong Cui 2003 *J. Micromech. Microeng.* **13** 430

View the [article online](#) for updates and enhancements.

### Related content

- [Novel fabrication process for a monolithic PMMA torsion mirror and vertical comb actuator](#)  
Satoshi Amaya, Dzung Viet Dao and Susumu Sugiyama
- [Micro XY-stage using silicon on a glass substrate](#)  
Che-Heung Kim and Yong-Kweon Kim
- [A micromechanical relay with electrostatic actuation](#)  
Robert Sattler, Peter Voigt, Helmut Pradel et al.

### Recent citations

- [Cell Morphology on Poly\(methyl methacrylate\) Microstructures as Function of Surface Energy](#)  
Matthias Katschnig *et al*
- [Developing a predictive model for nanoimprint lithography using artificial neural networks](#)  
Tahmina Akter and Salil Desai
- [Challenges and Issues of Using Polymers as Structural Materials in MEMS: A Review](#)  
Yunjia Li



**IOP | ebooks™**

Bringing you innovative digital publishing with leading voices to create your essential collection of books in STEM research.

Start exploring the collection - download the first chapter of every title for free.

# Fabrication of high-aspect-ratio polymer-based electrostatic comb drives using the hot embossing technique

Yongjun Zhao and Tianhong Cui

Institute for Micromanufacturing, Louisiana Tech University, 911 Hergot Avenue, Ruston, LA 71272, USA

E-mail: tcui@coes.latech.edu

Received 10 January 2003, in final form 24 February 2003

Published 18 March 2003

Online at [stacks.iop.org/JMM/13/430](http://stacks.iop.org/JMM/13/430)

## Abstract

We report on the formation of a lateral comb drive on poly-methyl-meth-acrylate (PMMA) using the hot embossing technique. A hot embossing mold insert is fabricated on a silicon wafer by means of lithography and inductive coupled plasma dry etching. The comb drive microstructure is hot embossed under a molding force of 35000 N at 130 °C. We demonstrate the comb drive, 80 units of interdigitated parallel capacitors with the finger gap and width both being 10  $\mu\text{m}$ . The minimum feature size is 5  $\mu\text{m}$  and the thickness of the structure is 60  $\mu\text{m}$ , which makes the aspect ratio 12:1. The comb drive strokes 5  $\mu\text{m}$  under an actuation potential of 180 V. We also present a brief description of the design and simulation with ANSYS.

## 1. Introduction

An electrostatic comb drive is one of the most important components in microelectromechanical systems (MEMS). A standard comb drive is formed by two sets of fingers with uniform gaps. Each pair of fingers forms a parallel capacitor. One set of fingers, called the fixed or stationary fingers, is fixed on the substrate. The other set, the so-called movable fingers, is free to move relatively to the fixed fingers. The movable fingers can move either laterally with the gaps fixed, or move vertically with the gaps closed to one side or the other.

Much research and development on varieties of comb drives have been published since the first report presented by Tang *et al* [1, 2]. Johnson and Warn [3] made a thorough analysis on the physics in their paper, 'Electrophysics of Micromechanical Comb Actuators'. Ye *et al* [4, 5] presented an 'optimal shape design of two- and three-dimensional comb drives', in which they proposed quadratic or cubic force profiles under constant bias voltage by the changing finger shape. Rodgers *et al* [6] presented an actuation system with large force, low voltage, and efficient area. Other investigations on the comb drive have also been published, including an asymmetric comb drive in out-of-plane and torsional motions [7], a comb drive with extended travel [8],

sub-micrometer gap comb drive microactuators [9], and an angular comb drive actuator [10].

Polymer materials have been of great interest in the research and development of integrated circuits (IC) and MEMS recently due to their relatively low cost and much easier processing. Hot embossing of polymers is a promising alternative to the traditional silicon processes. It fulfills the demand for the low-cost methods for mass production of microcomponents and microsystems. The polymer materials for hot embossing are much cheaper than silicon wafers. For hot embossing of polymer materials, complex micromachining steps are only necessary to fabricate a master mold. Once the master mold is completed, the desired microstructures can be easily batch replicated by the hot embossing process.

Hot embossing is essentially the stamping of patterns into a polymer by raising the temperature above the polymer's glass transition point. During the past several years, hot embossing technology has been developed and applied to both laboratories and industries in a variety of fields. For example, hot embossing lithography (HEL) has been proposed as one of the most promising methods to replace e-beam or x-ray lithography, as the feature size is scaled down to nanometers for large area and mass production. In HEL, a master mold can be made by e-beam lithography and proper etching processes. Next, the nano-patterns are batch imprinted on the large-scale

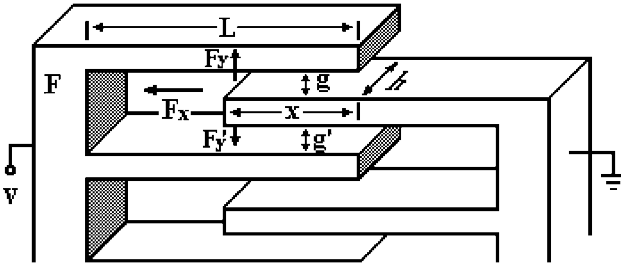


**Figure 1.** Partial schematic diagram of a standard driven comb drive.

substrates by hot embossing [11–13]. Hot embossing has been well applied to the fabrication of microfluidic devices on poly-methyl-meth-acrylate (PMMA) substrates for analytical chemistry and biomedical applications such as micro total analysis systems ( $\mu$ -TAS), i.e. the lab-on-a-chip [14, 15]. As mentioned previously, polymer microfabrication by hot embossing is also becoming increasingly important as a low-cost alternative to silicon or glass-based MEMS technologies [16–20].

In this paper, we present a polymer-based comb drive with high aspect ratio, which has been implemented successfully using the hot embossing technique. We also report on the corresponding design and simulation with ANSYS for polymer-based interdigitated comb microstructures.

## 2. Design of comb drive microstructures

### 2.1. Pull-in problem on the end fingers

A lateral comb drive moving in the  $x$ -direction is designed for the first experiment. To design a comb drive on PMMA, it is necessary to pay more attention to the issues of the pull-in voltage and stability because PMMA is much ‘softer’ than silicon.

Figure 1 illustrates several units of a standard comb drive. It also shows the coordinates and symbols used in the design and simulation. From figure 1, we can see that there is a substantial driving force in the  $y$ -direction, the so-called gap-closing driving force, between the two fingers because the gap is normally very small. If the movable fingers remain precisely at the center between two neighboring fixed fingers, the gap-closing driving force is counteracted. However, the gap-closing driving force at the end fingers cannot be balanced. Therefore, if the voltage is high enough or the end fingers are very thin, the fingers will be deflected significantly. In an extreme case, the fingers will be clamped together, resulting in a circuit short and breakdown, which is called the pull-in problem.

The direct evaluation of the relationship between voltage and deflection is difficult due to the coupled multiple physical fields. The attractive force from the electrostatic field results in the deflection of the finger. The bent finger results in the increase of the electrostatic force, which leads to further deflection of the finger until the restoring elastic force of the finger balances the electrostatic force. Fortunately, there are commercial software programs available to solve these types of problems. In our research, we used ANSYS 5.7 from the ANSYS Company.

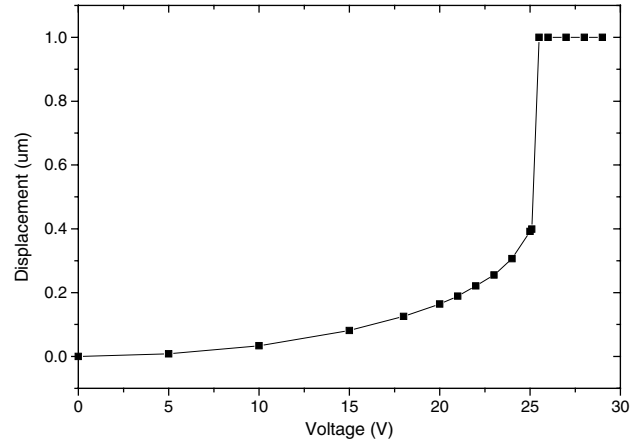


**Figure 2.** The relationship between bias voltages and deflections. Finger length  $L$  is  $20 \mu\text{m}$ , gap and finger thickness are both  $1 \mu\text{m}$ , and overlapped length is  $10 \mu\text{m}$ .

A two-dimensional model in ANSYS is used to simulate the pull-in problem due to the linear relationship between the bending moment and the electrostatic force in the  $h$ -direction. The medium surrounding the fingers is meshed as air with the relative permittivity of 1. The bent finger is meshed as a polymer beam with Young’s modulus of  $3 \times 10^9 \text{ Pa}$  and Poisson’s ratio of 0.34. The movable finger is not meshed because it is an equipotential body. The voltage is applied to the outer surfaces of the two fingers. As shown in figure 2, the pull-in occurs at a voltage of about 25 V for the given microstructure. For the same structure on silicon, the pull-in voltage is about 190 V. Compared with silicon, polymer is more flexible as a sensor or actuator material due to the lower pull-in voltage.

### 2.2. Stability

We should note that a comb drive is an inherently unstable system. As mentioned previously, there is a substantial driving force among the fingers in the  $y$ -direction. The gap-closing driving force is balanced only when the moving fingers remain precisely at the center between the two neighboring fixed fingers. Any perturbation of the center fingers will cause an offset of the force and pull the fingers to one side or the other.

The key point to design a stable comb drive is to make sure that the energy stored in the  $y$ -direction is much higher than that in the  $x$ -direction, i.e. the relationship,  $K_y \gg \frac{x^2 K_x}{g^2}$ , has to be satisfied, where  $K_y$  and  $K_x$  are the spring constants in the  $y$ - and  $x$ -directions, respectively.

### 2.3. Constant force range

One of the most important features of a lateral comb drive is that a constant driving force with a large stroke distance under a constant bias voltage can be achieved. This linear relationship provides us with many benefits to design varieties of microsensors or microactuators. However, this constant force feature is no longer sustained when the moving fingers stroke close to the support beam of the fixed fingers. Now the capacitance between the cross section of the movable finger’s

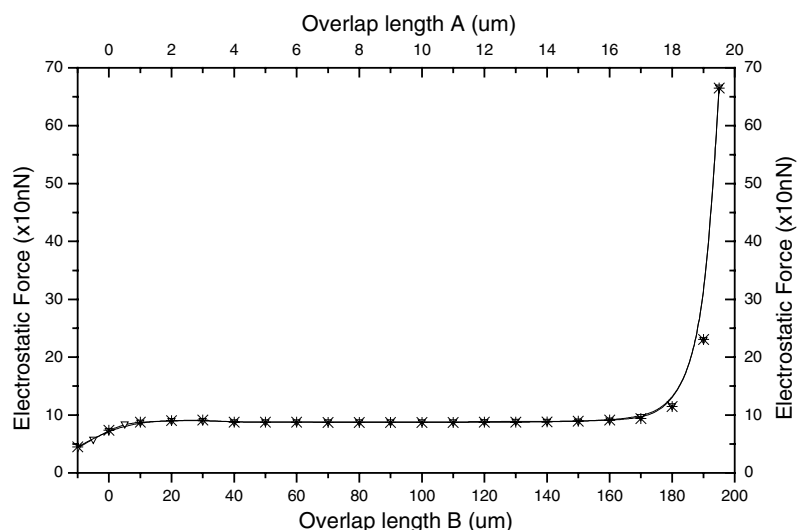


**Figure 3.** Drive force versus the overlapped length. Structure A:  $L = 20 \mu\text{m}$ ,  $d = g = 1 \mu\text{m}$ ,  $h = 1 \mu\text{m}$ ; Structure B:  $L = 200 \mu\text{m}$ ,  $d = g = 10 \mu\text{m}$ ,  $h = 10 \mu\text{m}$ .  $V = 10 \text{ V}$  in both cases.

end and the inside wall of the support beam of the fixed finger is significant. This relationship was also investigated with ANSYS.

This time, the three-dimensional (3D) model is used because there are only two 3D elements for the p-method simulation in ANSYS. With the p-method, good results with a desired accuracy can be obtained without rigorous user-defined meshing controls. In a p-method simulation, the global or local convergence criterion is specified to the desired physical quantity. The p-method employs higher-order polynomial levels (p-levels) of the finite element shape function selectively to approximate the real solutions. The required accuracy can be easily obtained by this method.

Two sets of results from different structures with the same scale ratio are illustrated in figure 3. This shows that for a comb drive with the same gap and finger width of  $g$ , the linear region starts from an overlapped length of  $2g$ , and stops at  $3g$  before the moving finger tips laterally reach the ends of sidewalls.

#### 2.4. Structure design

Processing limitations should also be taken into consideration in addition to the physical parameters when a comb drive system is designed. The main processing limitations come from: (a) the aspect ratio limitation for trench etching with vertical sidewalls in inductive coupled plasma (ICP) dry etching; (b) the aspect ratio limitation for the metallization on the sidewalls of fingers in the sputtering process because the metal atoms cannot attach to the bottom parts of sidewalls if the aspect ratio is too high; and (c) the aspect ratio limitation of the hot embossing process. In our experiments, the comb drive is one part of a tunneling accelerometer. The spring constant and the mass of the comb drive's movable parts also have to be considered. Finally, the structure's key dimensions, the finger width and gap, are both  $10 \mu\text{m}$  with the thickness of  $60 \mu\text{m}$ . This realizes a displacement of  $5 \mu\text{m}$  by 80 comb drive units at a bias voltage of 200 V in the simulated result.

All the corners on the structures are rounded. On one hand, this is required by the ANSYS simulation. In ANSYS,

in order to obtain the driving force, it is necessary to apply Maxwell force flags to the surfaces of the desired components; in our case, the movable fingers. ANSYS calculates forces by the approach of the Maxwell stress tensor. The total force applied to the desired components is achieved by summing the forces on each node of the flagged elements. If the corners are squares, the Maxwell stress tensor cannot accurately capture the concentrated force at the corner of the finger. This will result in a numerical simulation value of the driving force about 30% less than the analytical value. By trimming the corners, we can easily achieve simulation values differing from analytical values within 2%. On the other hand, round corners are also required by the hot embossing process. PMMA is easily shrunk and stuck on the sharp corners of the mold insert. This will result in the failure of the demolding process.

### 3. Microfabrication of comb drives

#### 3.1. Mold fabrication

To achieve a microstructure on PMMA using the hot embossing process, we need to fabricate a mold insert first. There are mainly two types of mold inserts: a metal mold formed by electroplating and a silicon mold fabricated by dry or wet etching [17].

For the fabrication of a metal mold, the mold is electroplated in a nickel galvanic solution on a substrate with a layer of patterned photoresist. The electroplated nickel mold has several disadvantages: for example, it is prone to abrasion and wear; slow process; voids form in high-aspect-ratio structures; the LIGA process is complicated and expensive, etc.

Lithography and etching (wet or dry etching) are the simple processes needed to fabricate a silicon mold insert. Silicon molds have some advantages such as fast and low-cost fabrication, flat surface and suitable hardness, strength, and thermal conductivity. For the above reasons, we selected a silicon wafer as the mold insert with typical ICP dry etching. The high-aspect-ratio trench with a sidewall profile at  $90^\circ$  can

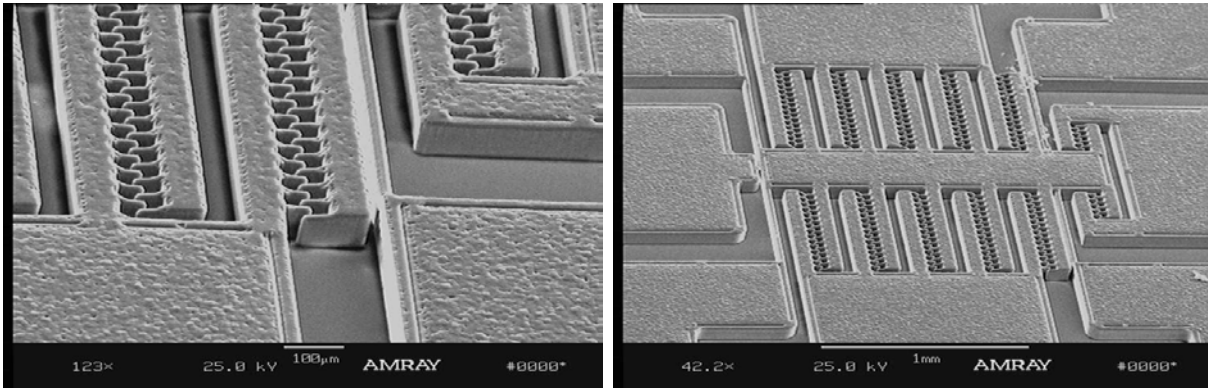


Figure 4. Hot embossing structures on PMMA.

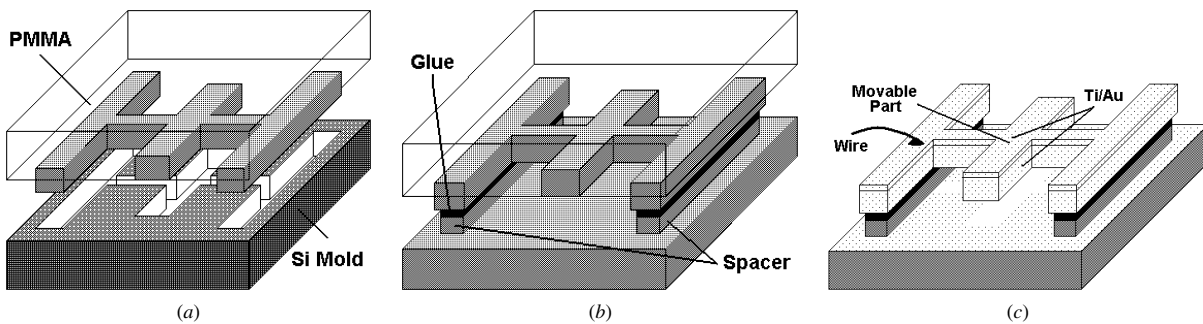


Figure 5. (a) Silicon mold and hot embossing on PMMA. (b) Two substrates are bonded together. (c) Device releasing and metallization.

be achieved with ICP. The drawbacks of the ICP process are the area-dependent etching and the micro-grasses formed at the trench bottom. In order to remove the micro-grasses, the wafer was soaked in the standard KOH solution at 70 °C for several minutes.

### 3.2. Hot embossing

The hot embossing system (HEX 01/LT, a commercial system from Jenoptik Mikrotechnik Company in Germany) is used in our experiments. The PMMA sheet is 0.5 mm thick with a glass transition temperature of 98 °C. The entire fabrication procedure and parameters are as follows:

- (1) open chamber and put PMMA on the substrate stage;
- (2) close chamber and evacuate it to 3 mTorr;
- (3) lower the mold to just touch the PMMA with the touch force of 300 N;
- (4) heat mold and PMMA at the same time to 130 °C and maintain this temperature for about 5 min;
- (5) insert the mold into PMMA under the molding force of about 35000 N and maintain for 1 min;
- (6) cool the mold and PMMA to 85 °C;
- (7) vent chamber and then demolding.

The whole processing cycle is about 20 min. Figure 4 shows a good result obtained by the above process.

### 3.3. Fabrication of bonding pads on a lower substrate

In order to make the movable part, the second PMMA substrate with bonding pads is fabricated. The bonding pads also serve as spacers. The spacer height is about 100 μm. The lateral

dimension of the spacer is 200 μm smaller than that of the electrode bonding pads of the comb drive so that the electrodes can be isolated from each other after the metallization process. The substrate with comb drive structures was flipped upside down and bonded onto the second PMMA substrate with epoxy. The whole process is illustrated in figure 5.

The spacers can be formed by either dry etching or hot embossing. Hot embossing is preferred because it is simple and fast. A metal masking layer is necessary for dry etching. Therefore lithography, metal deposition, and strip-off processes are necessary every time for the dry etching approach.

### 3.4. Releasing and metallization of movable parts

After the two substrates are bonded together, the next step is to release the movable parts of the comb drive. The back side of the PMMA substrate was etched all the way down to the comb drive. Because the total thickness is about 500 μm, fast removal of PMMA is necessary. First, PMMA was abraded and polished with fine sandpaper close to the structures at about 50 μm. An even thickness of 20–30 μm can easily be achieved with this abrading method because the PMMA is very soft. Next, the remaining PMMA was etched by reactive ion etching (RIE) using the gases O<sub>2</sub> and SF<sub>6</sub>. The etching rate is about 0.5 μm min<sup>-1</sup>. The microstructures of the movable comb drive are shown in figure 6.

Metallization is performed by sputtering Ti/Au = 300 Å/1000 Å after the structures are fully released. Next, wires are bonded on the bonding pads using conductive epoxy. Now the device is ready for characterization.

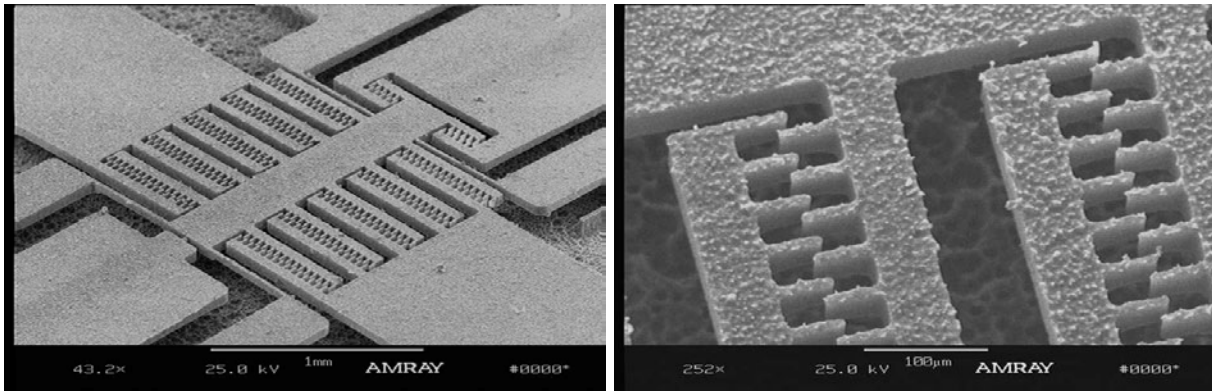


Figure 6. (a) The whole released comb drive structures. (b) Enlarged local area.

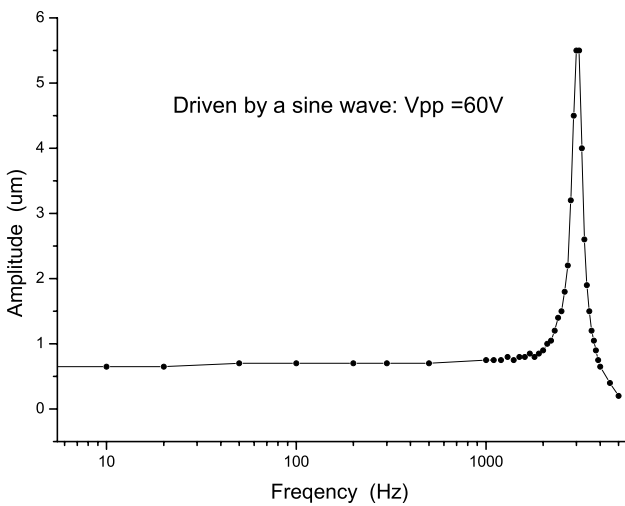


Figure 7. Measurement by a digital laser Doppler vibrometer. The natural frequency is about 3 kHz.

#### 4. Testing results

The comb drive is placed under a microscope with a CCD camera so that the microstructures can be seen on a monitor. A high voltage generator is connected to the comb drive. The vibration of the movable fingers can be checked clearly on the monitor, while the applied voltage changes. A fixed tip electrode is fabricated close to the suspension beam of the moving part. The initial gap between the tip and the beam is 5  $\mu\text{m}$ . Measurement shows that the suspension beam touches the tip under the applied voltage of about 180 V. This voltage value is very close to our simulation result.

The natural frequency of the comb drive is measured with the following procedure. The system is driven by a sine wave voltage with a  $V_{pp}$  of 60 V. The vibration of the moving fingers is measured by a digital laser Doppler vibrometer from Polytec Company. The results for our typical structures are shown in figure 7. The key dimensions of the structures are shown in figure 8. This measurement result also matches very well with the analytical calculation and numerical simulation. In the simulation of the resonant frequency with ANSYS 5.7, the quality factor  $Q$  has to be calculated analytically. The natural frequency of about 2.6 kHz is obtained from the harmonic

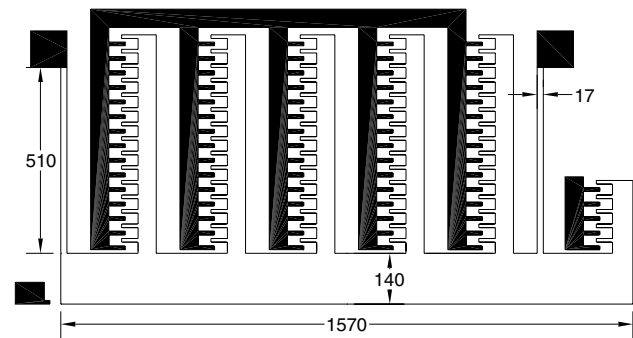


Figure 8. Half of the comb drive structures with key dimensions (units are  $\mu\text{m}$ ). The dark areas are fixed parts. The finger width and gaps between two figures are both 10  $\mu\text{m}$ .

response analysis with ANSYS 5.7 after the  $Q$  value of 503 calculated manually is input.

#### 5. Conclusions

A comb drive is successfully fabricated on PMMA by hot embossing for the first time. The test results match the simulation very well. Several advantages of this technique are observed in our experiments as follows:

- (1) the whole process is simple and low cost;
- (2) all the procedures are performed at low temperatures, usually below 130  $^{\circ}\text{C}$ ;
- (3) the PMMA structure has less stress and higher flexibility compared with the counterpart on silicon or poly-silicon;
- (4) the driving voltage is also much lower compared with silicon-based devices because PMMA has a lower Young's modulus.

Because this work is at an early stage, there is much room to improve the properties of polymer-based comb drives, such as reducing the actuation potential, increasing the stroke distance, and adjusting the natural frequency.

#### References

- [1] Tang W C, Nguyen T H and Howe R T 1989 Laterally driven polysilicon resonant microstructures *Tech. Dig. IEEE Micro Electro Mech. Syst. Workshop (Salt Lake City, 20–22 Feb. 1989)* pp 53–59

- [2] Tang W C 1990 Electrostatic comb drive for resonant sensor and actuator application *PhD Dissertation* University of California, Berkeley, CA
- [3] Johnson W A and Warn L K 1995 Electrophysics of micromechanical comb actuators *J. Microelectromech. Syst.* **4** 49–59
- [4] Ye W and Mukherjee S 1999 Optimal shape design of three-dimensional MEMS with applications to electrostatic comb drives *Int. J. Numer. Methods Eng.* **45** 175–94
- [5] Ye W, Mukherjee S and MacDonald N C 1998 Optimal shape design of an electrostatic comb drive in microelectromechanical systems *J. Microelectromech. Syst.* **7** 16–26
- [6] Steven R M and Kota S A new class of high force, low-voltage, compliant actuation systems Webpage [www.mems.sandia.gov](http://www.mems.sandia.gov)
- [7] Andrew Y J L, Hui C-Y and Tien N C 2000 Electrostatic model for an asymmetric comb drive *J. Microelectromech. Syst.* **9** 16–26
- [8] Chan E K and Dutton R W 2000 Electro-static micromechanical actuator with extended range of travel *J. Microelectromech. Syst.* **9** 321–8
- [9] Hirano T, Furuhashi T, Gabriel K J and Fujita H 1992 Design, fabrication, and operation of submicron gap comb-drive microactuators *J. Microelectromech. Syst.* **1** 52–9
- [10] Patterson P R *et al* 2002 A scanning micromirror with angular comb drive actuation *15th IEEE Int. Conf. MicroElectroMechanical Systems* pp 544–547
- [11] Roos N *et al* 2001 Nanoimprint lithography with a commercial 4 inch bond system for hot embossing *Proc. SPIE* **4343** 427–35
- [12] Heyderman L J *et al* 2001 Nanofabrication using hot embossing lithography and electroforming *Microelectron. Eng.* **57–58** 375–80
- [13] Scheer H-C *et al* 2001 Strategies for wafer-scale hot embossing lithography *Proc. SPIE* **4349** 86–9
- [14] Lee G-B *et al* 2001 Microfabricated plastic chips by hot embossing methods and their applications for DNA separation and detection *Sensors Actuators B* **75** 142–8
- [15] Becker H *et al* 1998 Microfluidic devices for  $\mu$ -TAS applications fabricated by polymer hot embossing *Proc. SPIE* **3515** 177–82
- [16] Becker H and Heim U 2000 Hot embossing as a method for the fabrication of polymer high aspect ratio structures *Sensors Actuators A* **83** 130–5
- [17] Becker H and Heim U 1999 Silicon as tool material for polymer hot embossing *Proc. MEMS 99* pp 228–31
- [18] Muller K-D *et al* 1999 3D diced microcomponents fabricated by multi-layer hot embossing *MME'99: Micromechanics Europe (Gif-sur-Yvette, France, 27–28 September)*
- [19] Roetting O *et al* 1999 Production of movable metallic microstructures by aligned hot embossing and reactive ion etching *Proc. SPIE* **3680** 1038–45
- [20] Liwei L *et al* 1996 Microfabrication using silicon mold inserts and hot embossing *Proc. Int. Symp. Micro Machine and Human Science* pp 67–71